BROOKHAVEN
NATIONAL LABORATORY

BNL-96386-2011-IR

Calculation of Design Parameters for an Equilibrium LEU Core in the NBSR

A.L Hanson & D.J. Diamond

September 2011

Nuclear Science & Technology Department

Brookhaven National Laboratory

U.S. Department of Energy
National Nuclear Security Administration
National Institute of Standards & Technology

DISCLAIMER

This report was prepared as an account of work sponsored by an agency of the United States Government. Neither the United States Government nor any agency thereof, nor any of their employees, nor any of their contractors, subcontractors, or their employees, makes any warranty, express or implied, or assumes any legal liability or responsibility for the accuracy, completeness, or any third party's use or the results of such use of any information, apparatus, product, or process disclosed, or represents that its use would not infringe privately owned rights. Reference herein to any specific commercial product, process, or service by trade name, trademark, manufacturer, or otherwise, does not necessarily constitute or imply its endorsement, recommendation, or favoring by the United States Government or any agency thereof or its contractors or subcontractors. The views and opinions of authors expressed herein do not necessarily state or reflect those of the United States Government or any agency thereof.

TECHNICAL REPORT

Calculation of Design Parameters for an Equilibrium LEU Core in the NBSR

Date: September 29, 2011

Prepared by: A.L. Hanson and D.J. Diamond

Nuclear Science and Technology Department
Brookhaven National Laboratory
Upton, NY 11973

Prepared for
National Nuclear Security Administration and
National Institute of Standards and Technology

ABSTRACT

A plan is being developed for the conversion of the NIST research reactor (NBSR) from high-enriched uranium (HEU) fuel to low-enriched uranium (LEU) fuel. Previously, the design of the LEU fuel had been determined in order to provide the users of the NBSR with the same cycle length as exists for the current HEU fueled reactor. The fuel composition at different points within an equilibrium fuel cycle had also been determined. In the present study, neutronics parameters have been calculated for these times in the fuel cycle for both the existing HEU and the proposed LEU equilibrium cores. The results showed differences between the HEU and LEU cores that would not lead to any significant changes in the safety analysis for the converted core. In general the changes were reasonable except that the figure-of-merit for neutrons that can be used by experimentalists shows there will be a 10% reduction in performance. The calculations included kinetics parameters, reactivity coefficients, reactivity worths of control elements and abnormal configurations, and power distributions.

ACKNOWLEDGEMENTS

The authors appreciate the close cooperation with the staff at the National Institute for Standards and Technology (NIST), NIST Center for Neutron Research (NCNR). Without the support of Sean O'Kelly, J. Michael Rowe, and Robert Williams at NCNR this work would not have been possible. We also appreciate the important administrative support received from Lynda Fitz.

TABLE OF CONTENTS

LIST OF FIGURES

LIST OF TABLES

1. INTRODUCTION

The conversion of the NIST research reactor (NBSR) from high-enriched uranium (HEU) to low-enriched uranium (LEU) fuel necessitates a redesign of the reactor fuel. The change will occur only in the composition and thickness of the fuel and the thickness of the aluminum cladding. The overall geometry of the fuel plates and the assemblies will remain as in the present HEU core. The new fuel will be a foil of U10Mo, a uranium alloy with 10% molybdenum by weight. In order to determine the thickness of the foils in the fuel plates, neutronic calculations were carried out as a function of fuel burnup for an equilibrium LEU core [1]. These calculations led to a specific foil thickness that will support a 38.5-day equilibrium fuel cycle, with the shim arms completely withdrawn at the end of the cycle. This is a fundamental requirement for the converted core. The analysis was carried out with the same methodology that had been shown to be valid for the HEU core [1].

The objective of the current study is to take the new fuel design and determine the important neutronic parameters during an equilibrium fuel cycle and compare these properties with those for an equilibrium HEU core. Examples of these parameters are fundamental core properties like power distribution and shim arm worth, quantities necessary for safety analyses to be done in the future like reactivity coefficients and shutdown margin, as well as the figure-of-merit for providing neutrons to experimenters.

The development of the model used for the Monte Carlo neutronics calculations is explained in Section 2. This includes a description of the core and the methodology used to obtain the neutronics parameters. Section 3 provides results for the equilibrium core along with comparisons with the HEU core parameters obtained previously with the same methodology. This includes results for fuel composition, kinetics parameters, reactivity parameters, power distributions, and neutron beam performance. References are found in Section 4.

2. CALCULATIONAL METHODOLOGY

2.1 Description of the NBSR

In order to understand the methodology, one must first understand how the NBSR is constructed. Presently the NBSR is fueled with HEU; the enrichment being a nominal 93%. The fuel is U_3O_8 in an aluminum dispersion clad in aluminum. Since the reactor is cooled and moderated with D_2O, the fuel elements can be placed in a "loose" configuration, i.e. with significant space between each fuel element. Each fuel element has a 7-inch gap at the mid-core. This arrangement allows for the beam tubes to point directly to the middle of the core while having no direct line-of-sight with the fuel.

Each fuel element is constructed of 17 plates in each upper and lower half (34 plates per fuel element) and is constructed in the MTR curved plate geometry. Each plate is 13 inches long with 11 inches of fuel. The thickness of fuel in each plate is 0.02 inch,

equivalent to a volume of 296 cm^3 (18.1 in^3) of fuel per fuel element. This results in each fuel element having 350 grams of ^{235}U. The aluminum cladding is 0.015 inch thick on each side.

Figure 2.1 shows a planar view of the NBSR at the core midplane with some of the key structures identified. North and south are top and bottom of the page, east to the right and west to the left. The new cold neutron source (CNS) being placed in beam tube #9 is shown as well as the existing CNS that has been in service for many years. There are four cadmium shim arms that are rotated through the core in a semaphore fashion. Two pivot from the east and two pivot from the west. At the end of the fuel cycle, they are fully withdrawn from the core in a horizontal position and at shutdown they are inserted at an angle of 41° from horizontal.

In the startup position, the shim arms are partially inserted in the top half of the core and are slowly removed from the core during a cycle. This causes an asymmetry in the uranium burn between the top and bottom halves of the core. There is also an asymmetry between the east and west halves of the core due to asymmetries external to the core along with the semaphore motion of the shim arms. With thirty fuel elements in the NBSR, a model with 60 different materials allows each half fuel element to have its own inventory (fuel composition) and no symmetry is forced across the core. This model with 60 different materials imposes the assumption that the inventory is uniformly distributed within each material (half fuel element).

Figure 2.2 shows how the positions in the NBSR core are identified. The positions have 13 lettered columns and seven numbered rows. The space denoted with <RR> is the position of the regulating rod and the six positions denoted with <> are the 3½-inch in-core irradiation thimbles. These thimbles are aluminum tubes assumed to be filled with D_2O only. The four 2½-inch in-core irradiation thimbles located in positions D4, G3, G5, and J4 are not included in Figure 2.2, but are included in the neutronics model as evidenced in Figure 2.1. There is ~6.2 inches of spacing between the rows and ~3.6 inches between the columns.

The fuel management scheme for the NBSR is shown in Figure 2.3. Each fuel position is identified with two numbers and one letter. The letters are either E or W for the east or west side of the core noting that a fuel element always stays in the east side or in the west side of the core. Since there are thirty fuel elements, 16 stay in the core for eight cycles and 14 stay in the core for seven cycles. The first number denotes how many cycles the element will be in the core (either eight or seven) and the second number denotes the cycle in which the fuel element resides. Therefore at the beginning of a cycle, the 8-1 and 7-1 fuel elements are fresh, unirradiated fuel elements, and 8-8 and 7-7 are in their final cycles and will be removed after the cycle is over. After a cycle is finished the 8-8 and 7-7 fuel elements are removed and the 8-7 elements are moved into the 8-8 positions, the 7-6 elements are moved into the 7-7 positions. Likewise the 8-6 and 7-5 fuel elements are moved into the 8-7 and 7-6 positions, respectively. This keeps occurring until the 8-1 and 7-1 fuel elements are moved into the 8-2 and 7-2 positions and new, unirradiated fuel is placed in the 8-1 and 7-1 positions.

2.2 Determination of Fuel Element Compositions

The methodology for determining the fuel nuclide inventories for the 2004 Safety Analysis Report (SAR) [2] is documented elsewhere [3]. That analysis was performed using the MONTEBURNS [4] program which utilizes the MCNP [5] and ORIGEN2 [6] computer codes. In recent years, the methodology for generating inventories with MONTEBURNS has been incorporated as the BURN option of MCNPX v2.6.0 [7] and some of the capabilities expanded. MCNPX makes use of the CINDER'90 [8] code instead of ORIGEN2 for solving the burnup equations. It is this methodology that has become the standard for NBSR analysis [1].

The analyses performed for the SAR had been shown to be valid because it satisfies the constraints imposed, namely the initial and final (fully withdrawn) measured shim arm positions give a multiplication factor (k_{eff}) of unity, within an acceptable uncertainty. Those results have also been shown to provide shim arm reactivity worths consistent with measurements. In [1] the differences and similarities that arose from the different methodologies used for the SAR and for the present effort are quantified and discussed.

Some of the limitations that existed in the MONTEBURNS code, as discussed in [1], remain in the MCNPX code with the BURN option. The most important issue is that not every fission product can be included in the inventory. Any isotope that is not in the library of isotopes is ignored by MCNPX and MCNPX does not include any "representative" (or "lumped") fission product to make up the difference in the mass that is "ignored." MCNPX handles this issue by reducing the mass that is tracked in each material as CINDER'90 returns an isotope that MCNPX does not recognize. Therefore, in order to generate each inventory based on the relative mass of the material, the mass of each isotope is extracted and the "missing mass" is calculated. That mass is added to the mass of ^{133}Cs, as the "representative fission product". The isotope ^{133}Cs was selected since it is a stable fission product that is produced by the fission of all fissionable atoms so it is always present in the inventories of fission products.

It should be noted that when the ENDF/B-VI cross section libraries were used with the MONTEBURNS/MCNP codes, the unaccounted mass was reported to be ~1.2% per cycle per fuel material. Using the present ENDF/B-VII libraries, which contain more cross section files for fission products, the analyses resulted in unaccounted mass of ~0.13% per cycle per fuel material. The largest number is fission products that were generated for the inventories was 54 using MONTEBURNS with the ENDF/B-VI cross section files and 181 with MCNPX using the ENDF/B-VII cross section files.

The mechanics of developing inventories are given in [1, 9] and will not be reproduced here, though the calculational flow chart is reproduced in Figure 2.4 for reference. The inventories are developed for the equilibrium core at four different statepoints: The startup core (SU) has fresh fuel in four locations and in the irradiated fuel, all short-lived fission products such as xenon have decayed away during the period from shutdown of the previous core, whereas the beginning-of-cycle core (BOC) has short-lived neutron

poisons such as xenon at their equilibrium concentrations. The BOC occurs approximately 1.5 days into a new cycle. End-of-cycle is the point at which the shim arms are completely removed and a middle-of-cycle point (MID) is halfway between BOC and EOC.

The inventories that were calculated for the SAR used a similar methodology but had several significant differences including those mentioned in the first paragraph of this section. Instead of calculating the inventories at four different statepoints as was done for this analysis, only two statepoints were calculated using MONTEBURNS. The shim arms were set at one intermediate setting and the EOC inventories were generated. The short lived isotopes were decayed and those inventories became the SU inventories for the subsequent cycle. Another significant difference between the methodology used for the SAR and the methodology used here is that the analyses for the SAR assumed the NBSR has a 38-day cycle instead of the more normal 38.5-day cycle. As was discussed in [1], there were no significant changes in the key parameters that were calculated for the NBSR when using inventories calculated for a 38-day cycle vs. a 38.5-day cycle. Therefore, all of the calculations for the LEU core were based on a 38.5-day cycle.

The methodology for developing the equilibrium LEU inventories was identical to that for developing the inventories for the HEU fuel with the exception that there is a different fuel meat and different fuel and cladding thicknesses. The thickness of each fuel plate was maintained between the HEU fuel and the LEU fuel so the cladding for the LEU fuel will be thicker than the cladding presently used with the HEU fuel since the fuel meat with the U10Mo foil is thinner than with the dispersion fuel.

Using MCNPX with the BURN option is more flexible for calculating inventories than using the MONTEBURNS, MCNP, ORIGEN code package (noting that MONTEBURNS was not developed for the purpose of calculating inventories). Those differences and improvements are discussed in [1]. Reference [1] also pointed out the differences between the previous data whose inventories were calculated with the MONTEBURNS/MCNP/ORIGEN code package using ENDF/B-VI cross section files and those calculated with the MCNPX code using the ENDF/B-VII cross section files. In this report only the work using MCNPX with the ENDF/B-VII cross section files is presented.

The inventories were calculated with the MCNP geometry model of the NBSR, updated in 2010. The analysis utilized the MCNPX computer code with the BURN module using 60 materials and maintaining the 38.5 day cycle. As is implied from Figure 2.4, numerous sets of computer calculations were performed in order to determine that equilibrium was reached in the inventories for both the HEU and LEU fuels. For the HEU fuel more than 30 sets of calculations were performed and for the LEU fuel more than 20 sets of calculations were performed. Once a set of inventories has been developed, the k_{eff} was calculated for the EOC equilibrium condition. This condition is the "base case" for the subsequent analyses since it represents the only situation that will be identical in the NBSR between the HEU and LEU cores; i.e. the shim arms and

regulating rod are removed and there is no longer enough excess reactivity in the core to maintain criticality. At this point the NBSR shuts down. By definition, the value of k_{eff} is unity just before the reactor shuts down. However the calculations are not perfect so there is a bias in the calculations, which is the value of k_{eff} that is calculated by the MCNP code.

A 0.5-2% bias in MCNP calculations using the ENDFB-VII cross section libraries has been reported elsewhere [10]. For these calculations with the HEU fuel the bias is on the order of 0.6%. Since the only difference between the analysis of the HEU and LEU fuels is in the composition of the fuel, we have assumed that the bias will be similar between the HEU and LEU cores. The main differences between the fuels is (1) the enrichment for the HEU fuel is 93% and for the LEU fuel is 19.75%; (2) the HEU fuel has aluminum and oxygen in the fuel and the LEU fuel has molybdenum; (3) the cladding thickness is larger for the LEU fuel than it is for the HEU fuel; and (4) there are slightly more actinides in the LEU fuel than in the HEU fuel. As will be discussed below, the power from the fission of ^{235}U is ~100% for the HEU fuel and ~96% for the LEU fuel. The cross section libraries that were used are identical for the analysis of the two cores.

There is a slight difference between the uranium content presented here and the numbers presented in the previous report [1]. During the course of this program, a significant error was uncovered in the BURN module of the MCNPX computer program. After the preliminary report [1] was written, the final value of k_{eff} settled at 1.00611 for the HEU up from 1.005 reported in [1]. The effects of this change did not significantly change any of the results or conclusions presented in [1]. The predicted LEU ^{235}U content for the fresh, unirradiated LEU fuel is now 383 grams vs. 386 grams previously predicted, approximately a 1% difference. This is certainly within the accuracy of the calculation and there is no justification to make any changes to fuel specifications that have been developed for the LEU fuel based on the previous report. The difference between the 383 g fuel element that the calculations settled on versus the 386 g fuel element in the preliminary report is insignificant as will be shown below. However, the lower value was maintained for the neutronic analysis in order to maintain computational consistency between the HEU and LEU fuels. The fuel mass specifications are presented in Table 2.1. From the previous report [1] the width of the foil in the calculation was 0.02165 cm (0.008524 inch) for a volume of 63.0779 cm^3 (half-element). For the present working analysis the foil thickness was 0.0215 cm (0.008465 inch) for a volume of 62.6408 cm^3. The engineering specifications on fuel thickness will then be 0.0085 inch (which encompasses both the 383 and 386 gram fuel elements). The rolling tolerance is being quoted by the fuel developers as ±0.001 inch, so the fuel thickness will be specified as 0.0085 ±0.001 inch. The calculations of the key neutronic parameters likewise resulted in no significant differences between using either 383 or 386 grams of ^{235}U.

Because of the manufacturing tolerances discussed above the fuel will be specified as mass of the foil. However, there is also an uncertainty in the molybdenum content of the fuel [11]. Even though the specification is for U10Mo, the 10% weight specification for molybdenum has an uncertainty of ±1%. This effect produces a range in the ^{235}U

content of between 381 and 390 grams when the weight specification for ^{235}U is the nominal 386 grams. This is demonstrated in Table 2.2. Therefore both the 383- and 386-gram ^{235}U content is within the manufacturing tolerances if either value is specified. The ^{235}U content quoted in Table 2.2 assumes the enrichment is 19.75% and the density is 17.2 g/cm^3 with no variation.

Table 2.1 Fuel Specifications

	HEU	LEU [1]	LEU (present)
^{235}U grams	350	386	383
^{238}U grams	26	1567	1556
O grams	68	0	0
Al grams	625	0	0
Mo grams	0	217	215
Total grams	1069	2170	2154
Fuel density (g/cm^3)	3.612	17.2	17.2
Fuel thickness (cm)	0.0508	0.02165	0.02150
Fuel volume (cm^3)	148	63.0779	62.6408

Table 2.2 Effect of 1% Mo Variation on the 386 g Fuel Composition

	U10Mo	U9Mo	U11Mo
^{235}U	386	390	381
^{238}U	1567	1585	1550
Mo	217	195	239
Total	2170	2170	2170

The total ^{235}U content of the fuel elements as a function of cycle is shown in Figures 2.5 and 2.6 for the HEU and LEU fuel elements respectively. Cycle "0" represents the fresh, unirradiated fuel. Cycle "1" then represents the amount of ^{235}U present in the fuel at the end of the first cycle, and so forth. Figures 2.7 and 2.8 are the grams of ^{238}U in the fuel elements for the HEU and LEU fuels, respectively, and Figures 2.9 and 2.10 are the grams of ^{239}Pu in the fuel elements for the HEU and LEU fuels, respectively. Finally Figures 2.11 and 2.12 show the amount of other actinides in each fuel element as a function of cycle. The dominant isotope in the "other actinide" category is ^{236}U.

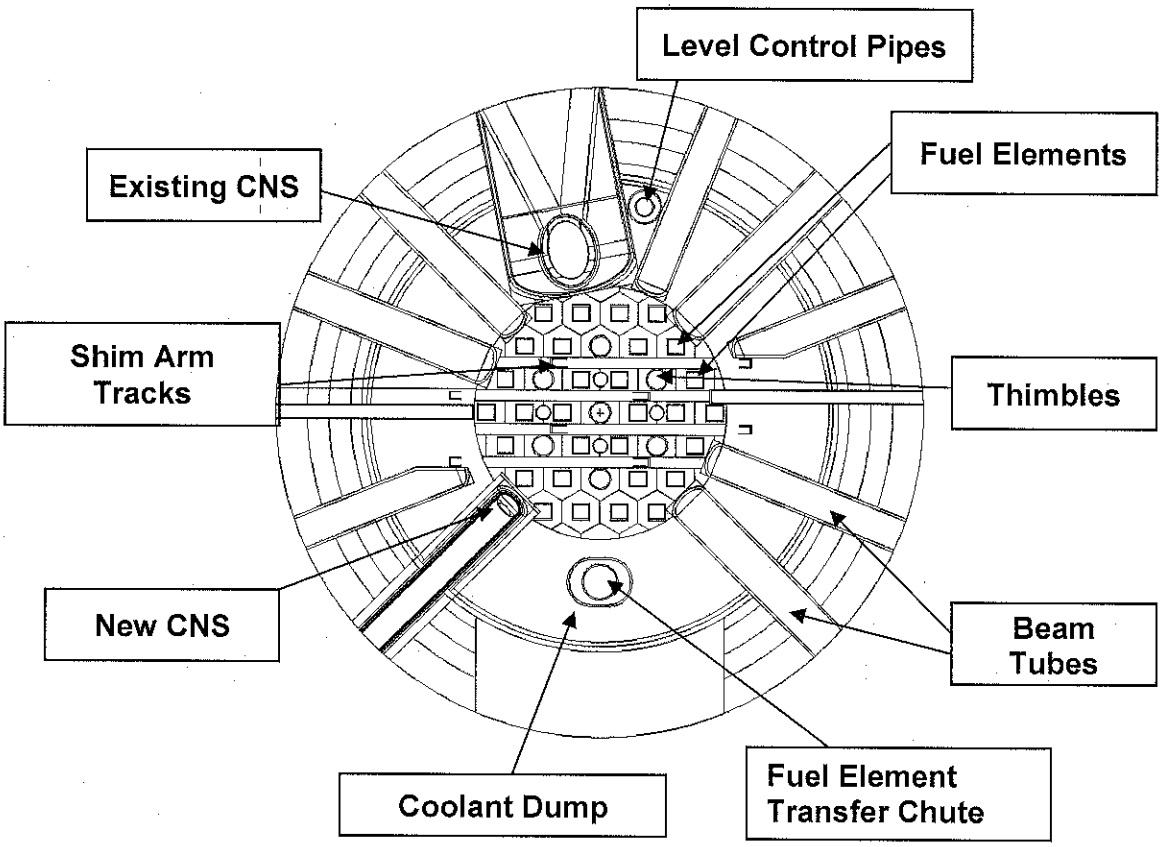

Figure 2.1 Planar View at Core Midplane

Figure 2.2 Fuel Element Position Designation

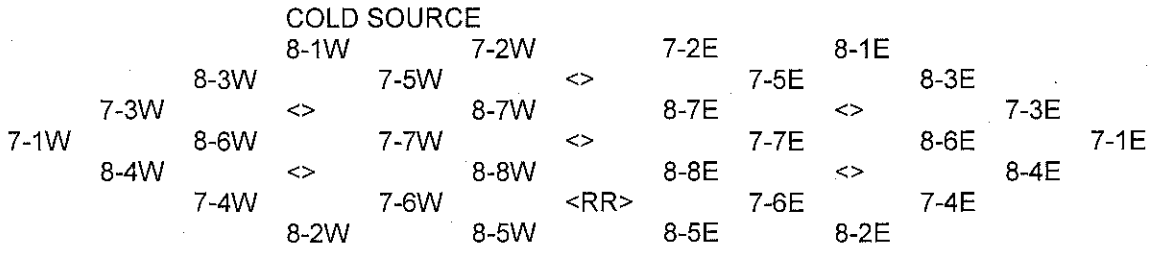

Figure 2.3 Fuel Management Scheme

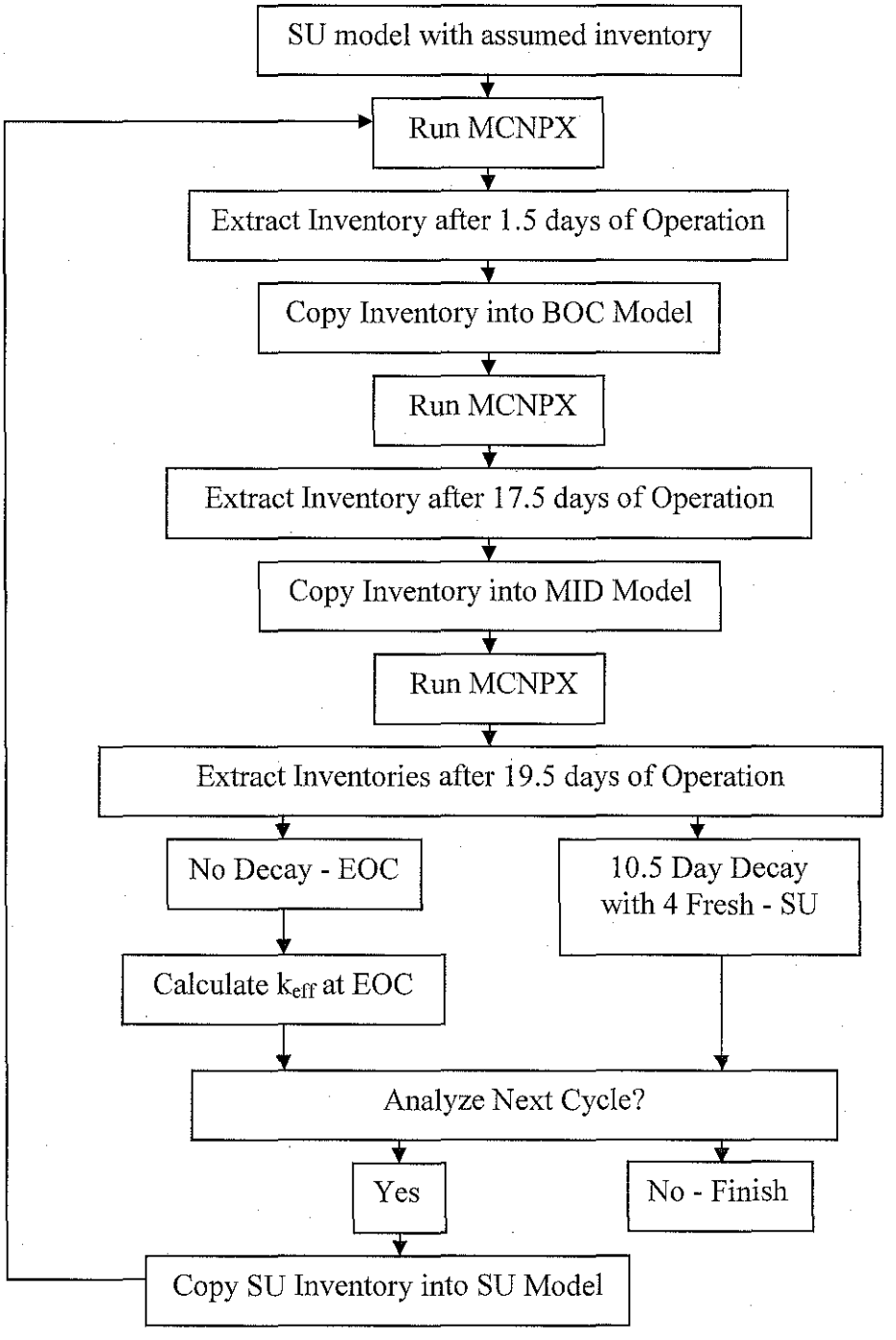

Figure 2.4 Flow Chart for the Methodology for Generating Inventories with MCNPX

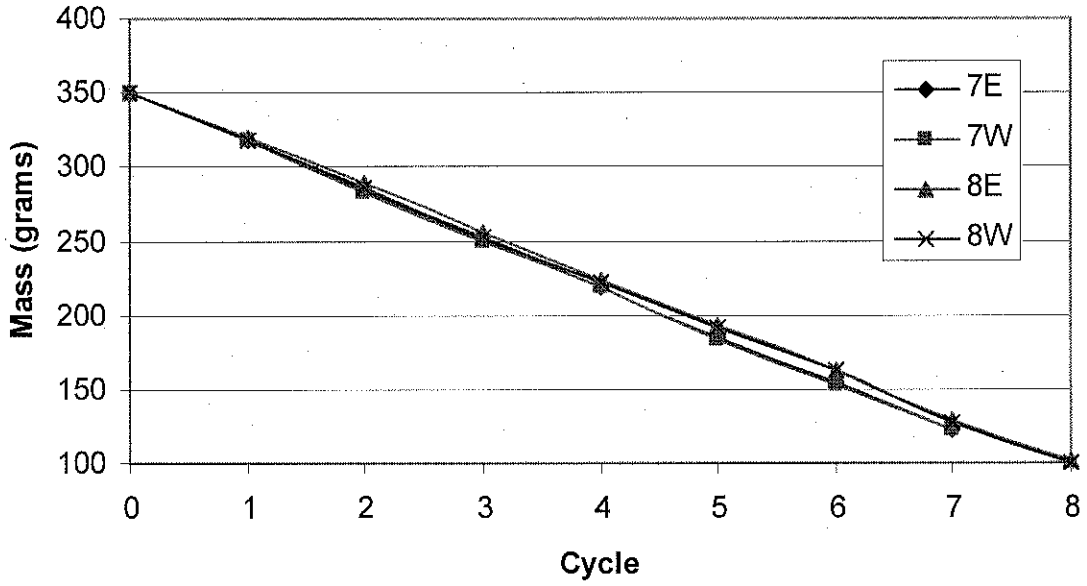

Figure 2.5 ^{235}U Content in Each Fuel Element as a Function of Cycle for HEU Fuel

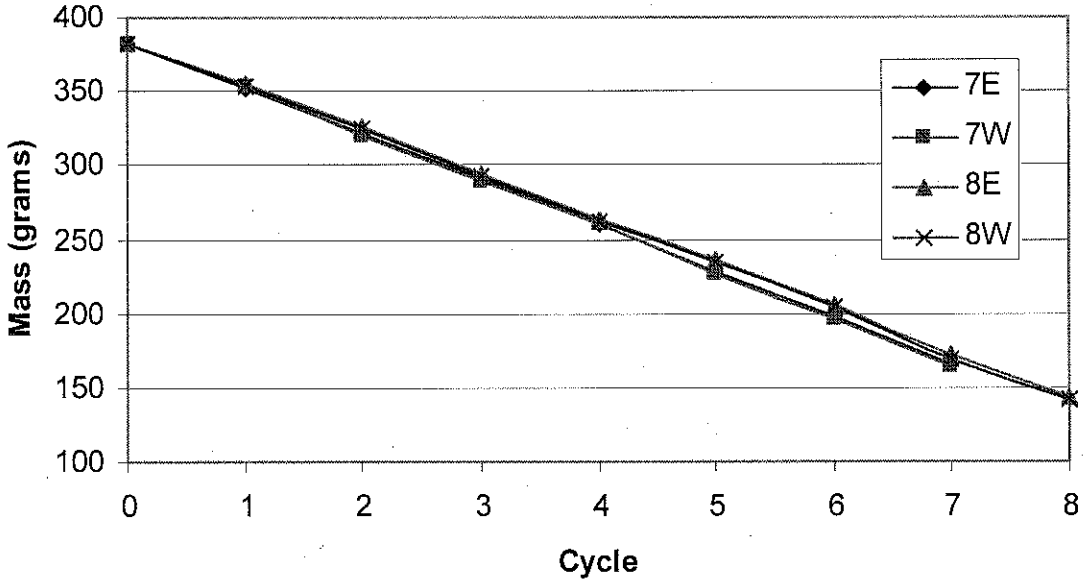

Figure 2.6 ^{235}U Content in Each Fuel Element as a Function of Cycle for LEU Fuel

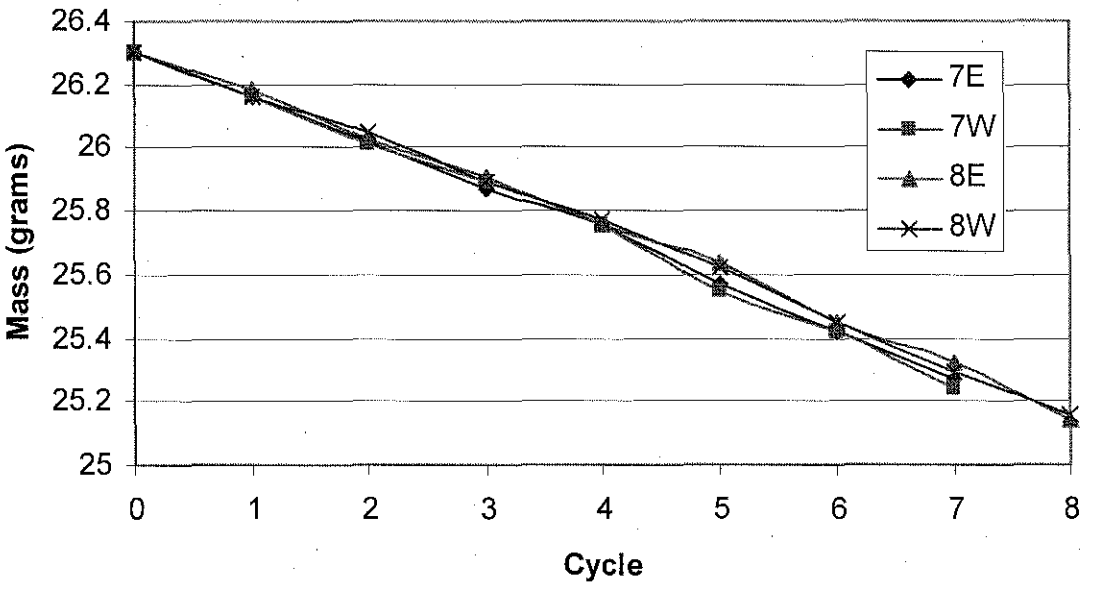

Figure 2.7 ^{238}U Content in Each Fuel Element as a Function of Cycle for HEU Fuel

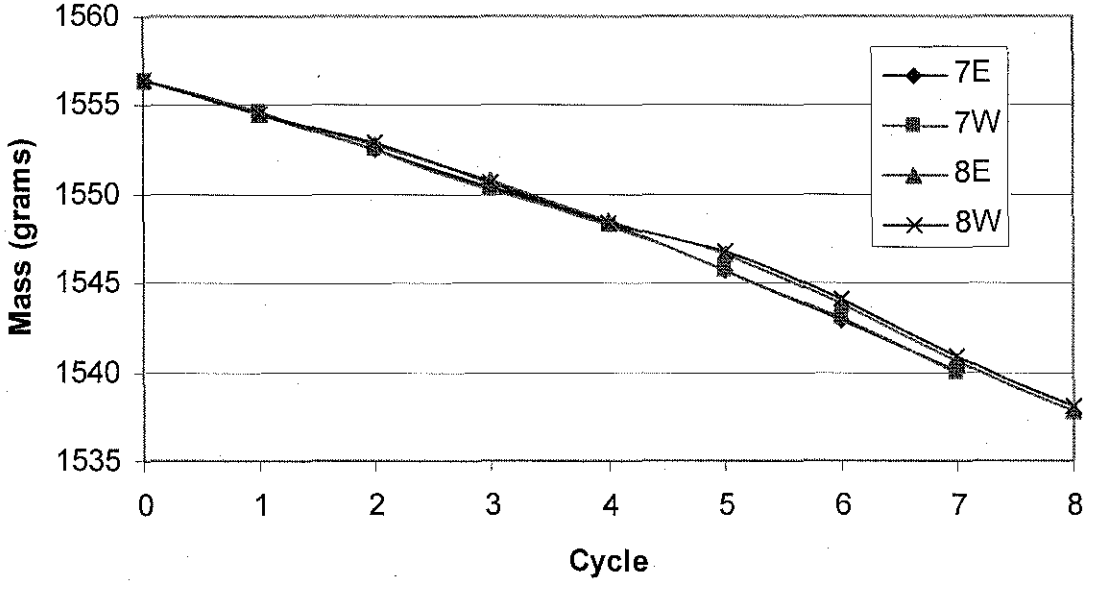

Figure 2.8 ^{238}U Content in Each Fuel Element as a Function of Cycle for LEU Fuel

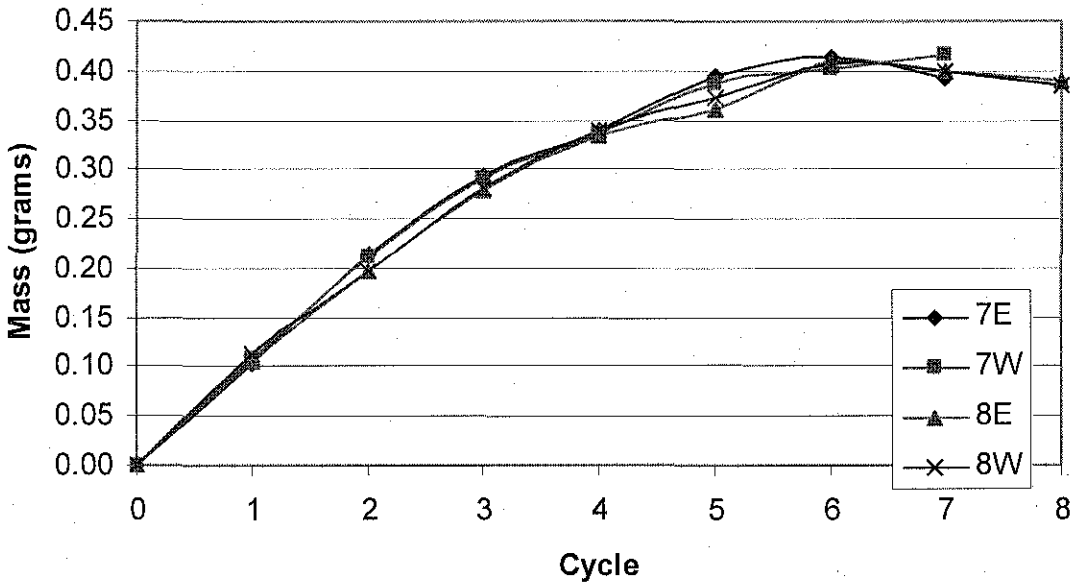

Figure 2.9 ^{239}Pu Content in Each Fuel Element as a Function of Cycle for HEU Fuel

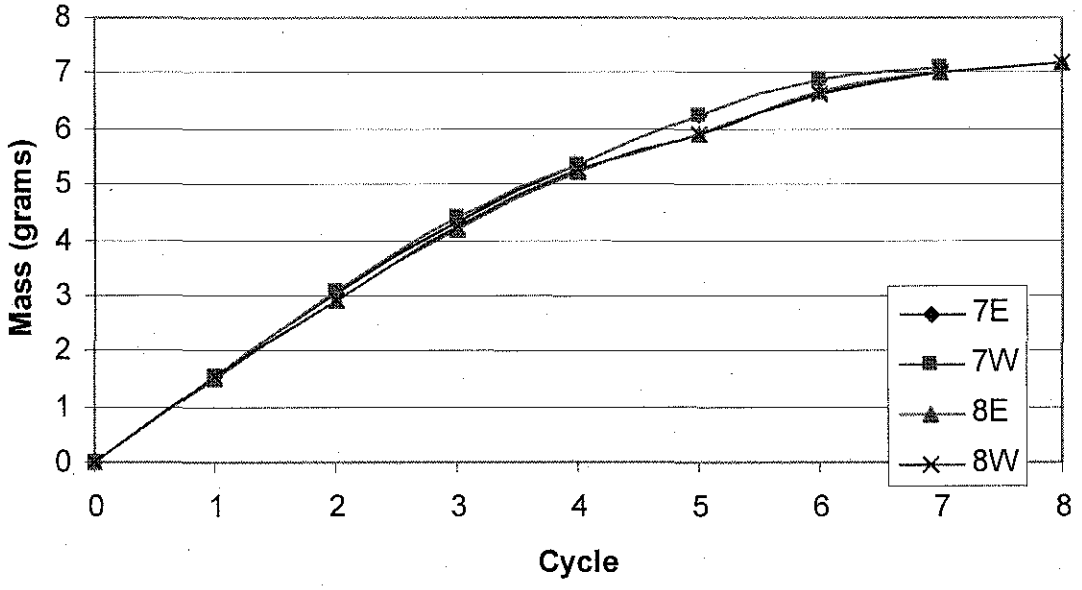

Figure 2.10 ^{239}Pu Content in Each Fuel Element as a Function of Cycle for LEU Fuel

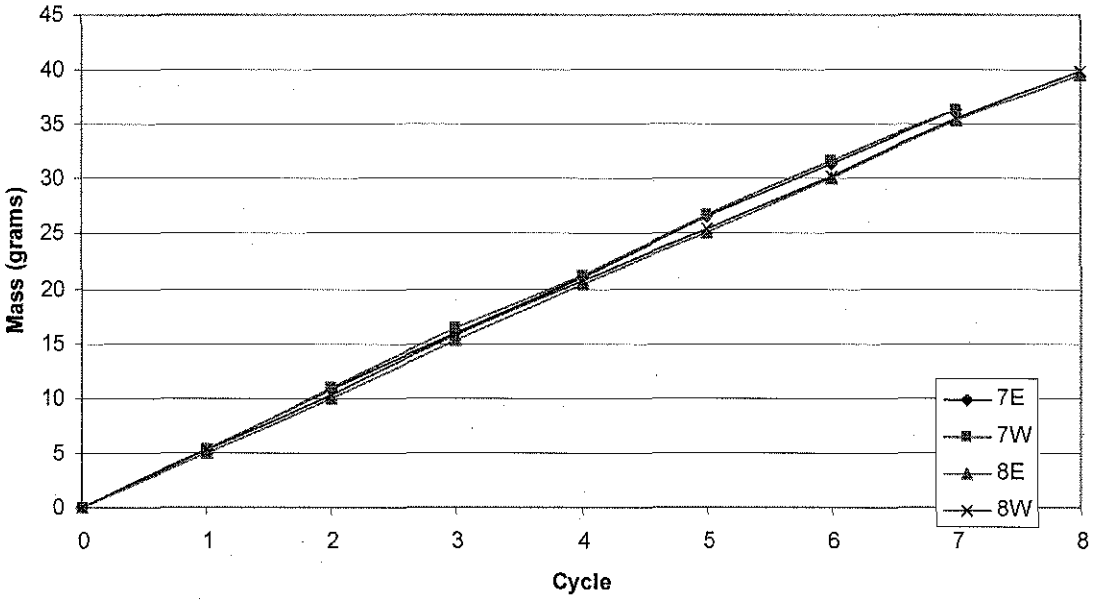

Figure 2.11 Content of all Other Actinides in Each Fuel Element as a Function of Cycle for HEU Fuel

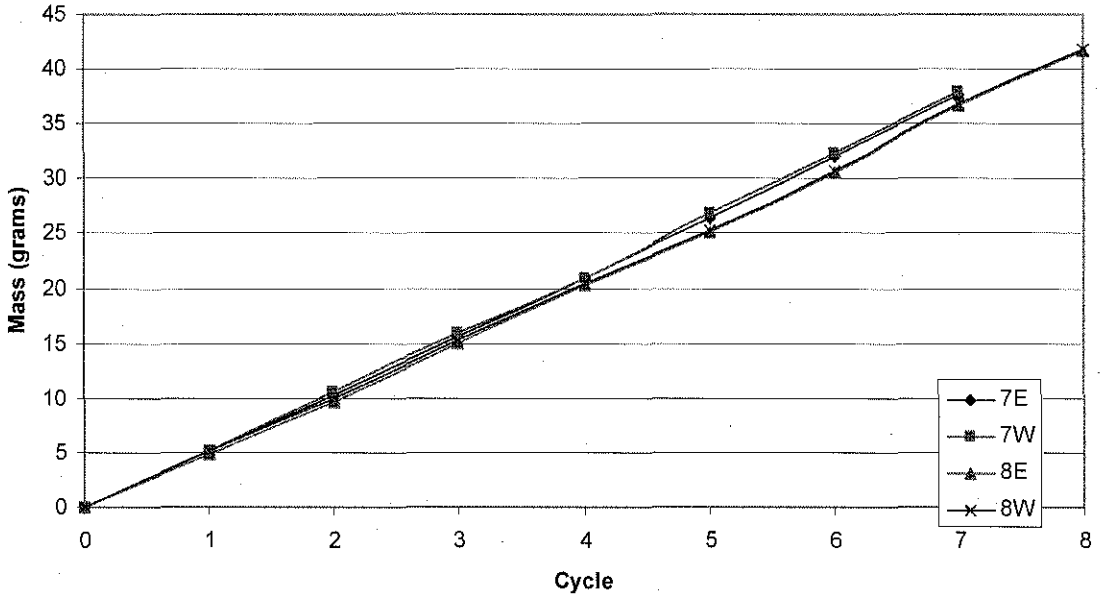

Figure 2.12 Content of all Other Actinides in Each Fuel Element as a Function of Cycle for LEU Fuel

3. CALCULATION OF PARAMETERS FOR THE LEU EQUILIBRIUM CORE

3.1 Actinide Buildup and Consumption.

One of the calculated parameters is the rate at which ^{235}U is burned during a cycle in each fuel element. Figures 3.1 and 3.2 show the amount (in grams) of ^{235}U burned in each fuel element during each cycle for the HEU and LEU fuels, respectively. The total ^{235}U burned in a cycle is calculated to be 954 grams for the HEU fuel and 919 grams for the LEU fuel. The difference in the ^{235}U consumption per fuel element between the HEU and LEU fuels are shown in Figure 3.3. The reason for the difference in the amount of ^{235}U burned between the HEU and LEU fuels is due to the burning of other actinides that build up in the LEU fuel. The contribution to the power from the fissioning of ^{238}U is calculated to be 0.01% in each fuel element for the HEU fuel and between 0.48% and 0.50% for the LEU fuel.

Figure 3.4 shows the distribution of the power contributed by the ^{239}Pu (in percent of the total power generated in each fuel element) for the HEU fuel and Figure 3.5 shows the distribution of the ^{239}Pu power contribution for the LEU fuel. The relative contributions in the power generation in each fuel element from the other actinides (other than ^{235}U, ^{238}U, and ^{239}Pu) are shown in Figures 3.6 and 3.7 for the HEU and LEU fuels, respectively. Over the entire core the power generated from ^{235}U is calculated to be 99.7% for the HEU fuel and 95.6% for the LEU fuel so the total fissionable material consumption is equivalent between the HEU and LEU cores.

3.2. Neutron Kinetics Parameters

The neutron lifetime is defined as the average time between the generation of prompt fission neutrons (which does not include delayed neutrons and photoneutrons) and when they are absorbed. For a D_2O cooled and moderated reactor such as the NBSR, the neutron lifetime will be longer than a reactor cooled and moderated with H_2O and is typically on the order of 700 μs.

The neutron lifetime for the NBSR has been calculated with two different methods. The first method is based on calculating the decay of neutrons when a hypothetical pulse of neutrons is inserted at the center of the subcritical core. This methodology is described in [12]. The other method uses the neutron lifetime calculation that has been recently included in MCNP5 [13]. The results for the lifetime for the HEU and LEU cores at SU and EOC are provided in Table 3.1. The results shown in Table 3.1 for the neutron lifetime at EOC agree well between the two methods. For the SU core, there is a larger difference between the two calculations, but the numbers are similar in magnitude. The uncertainties are based on MCNP5 statistics for those cases and on a more elaborate uncertainty analysis for the pulsed approach [12].

Table 3.1 Neutron Lifetime (in μs) as Calculated by MCNP5 and by Calculation of the Decay of a Pulse.

		SU	±	EOC	±
Pulse	HEU	744	35	819	48
MCNP	HEU	698	1	802	1
Pulse	LEU	860	44	771	40
MCNP	LEU	651	1	730	1

The delayed neutron fraction, β, is the number of neutrons that are either emitted by fission products or are photoneutrons (the result of a (γ,n) reaction) after the fission process has occurred, relative to the total number of neutrons emitted as a result of fission. In addition to knowing this fraction it is necessary to know the corresponding decay constant of the precursors to neutron emission. There are many neutron-rich isotopes that decay with the emission of neutrons so it is common to lump the precursors from fission products into six groups to simplify the representation with each group having an average half-life, or decay constant, λ_i an average fraction, β_i and a representative energy E_i of neutron emission. Since every fissionable isotope has its own set of fission products, the mix of precursors in each group will depend on the fissionable material in the reactor and will also depend on the neutron spectra.

Several different tabulations exist that provide estimates of both the representative half-life and magnitude and the values in the tabulations can vary significantly [14]. The values calculated by MCNP5 (for delayed neutrons from fission products) with the ENDF/B-VII cross section files are given in Table 3.2 for both the HEU and LEU fuel at SU and EOC. Values of the statistical uncertainty are also provided. The values of β are similar for the HEU and LEU fuels and between the SU and EOC conditions. In all cases the number of fissions in the NBSR is more than 95% from ^{235}U as shown in Table 3.3, for both HEU and LEU fuel at SU and EOC so the values of β will be close to the values for ^{235}U alone.

Table 3.2 Delayed Neutron Group Characteristics

HEU Fuel at SU						
Group	β_i	σ	E_i (MeV)	σ	λ_i	$t_{½}$
1	0.00022	0.00001	0.403	0.001	0.0125	55.5
2	0.00111	0.00002	0.472	0.001	0.0318	21.8
3	0.00107	0.00002	0.442	0.001	0.109	6.34
4	0.00301	0.00003	0.557	0.000	0.317	2.19
5	0.00092	0.00002	0.518	0.001	1.35	0.512
6	0.00032	0.00001	0.542	0.002	8.64	0.0803
$\beta = \sum \beta_i$	0.00665	0.00005				
HEU Fuel at EOC						
Group	β_i	σ	E_i (MeV)	σ	λ_i	$t_{½}$
1	0.00021	0.00001	0.407	0.001	0.0125	55.5
2	0.00112	0.00002	0.472	0.001	0.0318	21.8
3	0.00110	0.00002	0.442	0.001	0.109	6.34
4	0.00302	0.00003	0.557	0.000	0.317	2.19
5	0.00087	0.00002	0.518	0.001	1.35	0.512
6	0.00030	0.00001	0.539	0.001	8.64	0.0803
$\beta = \sum \beta_i$	0.00662	0.00005				
LEU Fuel at SU						
Group	β_i	σ	E_i (MeV)	σ	λ_i	$t_{½}$
1	0.00020	0.00001	0.405	0.001	0.0125	55.5
2	0.00108	0.00002	0.473	0.001	0.0318	21.8
3	0.00105	0.00002	0.442	0.001	0.109	6.33
4	0.00301	0.00003	0.557	0.000	0.317	2.18
5	0.00085	0.00002	0.518	0.001	1.35	0.513
6	0.00030	0.00001	0.538	0.001	8.66	0.0801
$\beta = \sum \beta_i$	0.00649	0.00005				
LEU Fuel at EOC						
Group	β_i	σ	E_i (MeV)	σ	λ_i	$t_{½}$
1	0.00020	0.00001	0.404	0.001	0.0125	55.5
2	0.00109	0.00002	0.473	0.001	0.0318	21.8
3	0.00102	0.00002	0.441	0.001	0.109	6.33
4	0.00301	0.00003	0.556	0.000	0.317	2.18
5	0.00087	0.00002	0.517	0.001	1.35	0.513
6	0.00030	0.00001	0.541	0.001	8.65	0.0801
$\beta = \sum \beta_i$	0.00649	0.00005				

Table 3.3 Percentage of Fissions from the Major Actinides as Calculated by MCNPX.

	HEU SU	HEU EOC	LEU SU	LEU EOC
^{235}U	99.73	99.67	96.35	95.71
^{236}U	0.02	0.02	0.02	0.02
^{238}U	0.01	0.01	0.49	0.49
^{239}Pu	0.23	0.27	2.99	3.54
^{241}Pu	0.02	0.02	0.16	0.24

3.3 Shim Arm Reactivity Worth

The worth of the shim arms was calculated using the fuel inventories at startup and end-of-cycle and calculating k_{eff} as a function of shim arm position (moving all four of the shim arms together). The shim arm worth curves for the HEU and LEU fuels are shown in Figures 3.8 at SU and 3.9 at EOC. The shim arms with the LEU fuel have less total worth than the shim arms with the HEU fuel. This is demonstrated in Table 3.4, the total shim arm worth for the two fuels. The decrease in the calculated total worth was 3% for SU and 5% for EOC.

Table 3.4 Total Shim Arm Worth (%Δk/k) for the HEU and LEU Fuel.

	SU	EOC
HEU	24.9	27.2
LEU	24.2	26.0

3.4 Regulating Rod Reactivity Worth

The regulating rod is an aluminum rod located in the G6 position. It performs the automatic fine control of the reactivity between larger reactivity insertions when the shim arms are moved. As the uranium in the core fissions, excess reactivity is lost and that loss is compensated by a slow and continuous withdrawal of the regulating rod. When the regulating rod is nearly fully withdrawn the shims arms are moved outward and the regulating rod is re-inserted. The regulating rod works by adding a large volume of a weak absorber and displacing D_2O from the G6 position in the core when it is fully inserted. The worth curves for the regulating rod are shown in Figures 3.10 for the HEU and LEU at SU and 3.11for the HEU and LEU at EOC. The total worth is shown in Table 3.5.

Table 3.5 Total Regulating Rod Arm Worth (%Δk/k) for the HEU and LEU Fuel

	SU	EOC
HEU	.50	.45
LEU	.53	.43

3.5 Shutdown Margin and Excess Reactivity

NBSR Technical Specification 3.1.2, Reactivity Limitations, states that the core cannot be loaded such that the excess reactivity will exceed 15% Δk/k and it also states that the NBSR shall not be operated if it cannot be kept shutdown with the most reactive shim arm fully retracted. To determine if these conditions are met, k_{eff} was calculated under the following conditions: all shims inserted (shutdown reactivity), all shim arms withdrawn (excess reactivity), and three of the four shim arms inserted with the other withdrawn (shutdown margin). The calculations were done at the most limiting time in the cycle which is SU when the fuel is freshest and there is no xenon present.

The results for the calculations are shown in Table 3.6. This table demonstrates that neither the HEU nor the LEU equilibrium cores exceed the excess reactivity limit of 15% Δk/k. This table also shows that for both the HEU and LEU fuels the core can be maintained in a shutdown condition with the most reactive shim arm withdrawn; shim arm #3. Note that these calculations are for fresh (or with no significant burnup) cadmium shim arms.

Table 3.6 Shutdown Margin and Excess Reactivity (%Δk/k)

		HEU	LEU
Shutdown reactivity (all shim arms in)		-18.2%	-18.3%
SDM	Shim 1 out	-12.1%	-12.2%
SDM	Shim 2 out	-11.1%	-11.2%
SDM	Shim 3 out	-10.1%	-10.8%
SDM	Shim 4 out	-11.6%	-11.9%
Excess reactivity (all shim arms out)		6.7%	6.3%

3.6 Moderator Temperature Coefficients

The moderator temperature coefficient (MTC) should be negative so if there is an inadvertent power rise, and hence a heating of the moderator, there will not be a positive feedback causing a further rise in the power. MCNP handles temperature of the moderator in two ways. The first is by specifying the density of the moderator and the second is through the cross section file which provides a scattering kernel.

The density of the D_2O is a user input so it can be changed in a continuous manner in order to study the effects of moderator temperature on the performance of the NBSR. For the general MCNP model of the NBSR the density of the D_2O is 1.0977 g/cm^3, the density at 46°C (115°F).

The scattering kernel of the deuterium was selected to be 293.6 K (20°C). In the ENDF/B--VII cross section files the scattering kernels are in 50°C increments, so the next highest available scattering kernel for deuterium is for a temperature of 350 K (76°C). The 20°C scattering kernel was selected since it is closer to the actual nominal operating temperature than the 350 K scattering kernel.

The MTC is calculated using the two ways of representing temperature change. First the scattering kernel was changed from 293.6 K to 350 K. The value of k_{eff} and $\Delta k/k$ was calculated and then divided by the temperature change. Second, the density was changed from 46°C to 96°C in 10°C increments maintaining the 293.6K scattering kernel. For each temperature step the value of k_{eff} and $\Delta k/k$ was calculated and divided by the temperature change. The values of $\Delta k/k/°C$ were then averaged. The values of reactivity change per degree from the scattering kernel change are added to the values calculated with the density change. The results of the calculations for the HEU and LEU fuel at SU and EOC are presented in Table 3.7. The MTC results are similar for the HEU and LEU cores.

Table 3.7 Moderator Temperature Coefficient (%Δk/k/°C) for HEU and LEU Fuels at SU and EOC.

SU		
	HEU	LEU
By Scattering Kernel	-0.0083±0.0002	-0.0063±0.0003
By Density Change	-0.0215±0.0002	-0.0218±0.0003
Total	-0.0297±0.0003	-0.0280±0.0003
EOC		
	HEU	LEU
By Scattering Kernel	-0.0074±0.0002	-0.0045±0.0002
By Density Change	-0.0201±0.0002	-0.0183±0.0002
Total	-0.0275±0.0003	-0.0228±0.0003

3.7 Void Coefficients

As with the MTC, the void coefficient also needs to be negative. If a bubble forms somehow in the core (e.g., through boiling) there should be negative feedback to the power level. The formation of bubbles is modeled as a change in the density of the coolant and moderator. In the discussion of the MTC in Section 3.6 lowering the density of the moderator was shown to result in negative feedback so any process that results in the decrease in the density will likewise have negative feedback.

Creating a void within a fuel element or irradiation thimble was calculated for the following cases:

- void all 2.5-inch irradiation thimbles
- void all 3.5-inch irradiation thimbles
- void all irradiation thimbles
- void the 7-inch gap in the fuel elements (FEs)
- void all of the fuel elements within the upper and lower bounds of the fueled regions

One could create a void in an irradiation thimble by placing an experiment in the thimble, but there is probably no credible method to create any void in the fuel elements other than boiling due to flow blockage. The methodology for this analysis is similar to the methodology for calculating the MTC. The region is first voided, the reactivity change (Δk/k) calculated, and the reactivity change divided by the volume of the void. The results are presented in Table 3.8 in %Δk/k/liter for the HEU and LEU cores at SU and EOC. The results in Table 3.8 demonstrate that a void forming anywhere within the NBSR is expected to provide negative reactivity feedback. The magnitude of the feedback is similar for the HEU and LEU cores.

Table 3.8 Void Coefficients (%Δk/k/liter) for Voiding Specific Areas in the Core.

	HEU	LEU
SU		
4 2.5-in thimbles voided	-0.045±0.002	-0.044±0.002
6 3.5-in thimbles voided	-0.036±0.001	-0.037±0.001
All thimbles voided	-0.038±0.001	-0.039±0.001
All FE gaps voided	-0.027±0.001	-0.031±0.002
All FEs voided	-0.019±0.001	-0.018±0.001
EOC		
4 2.5-in thimbles voided	-0.034±0.001	-0.035±0.001
6 3.5-in thimbles voided	-0.030±0.001	-0.032±0.001
All thimbles voided	-0.031±0.001	-0.032±0.001
All FE gaps voided	-0.022±0.001	-0.023±0.001
All FEs voided	-0.022±0.001	-0.022±0.001

3.8 Power Distributions

The radial power distributions show the average power generated in each half fuel element. Figure 3.12 shows the radial power distribution for the upper and lower half cores for the HEU core at SU. The numbers are the relative power generated in each location in the core. The power distributions are normalized so that unity represents the average power in a half fuel element, i.e., 1/60 of the total core power (=1/3 MW).

Figure 3.13 shows the radial power distribution for the upper and lower half cores for the LEU core at SU. Figures 3.14 and 3.15 show the power distributions at EOC for the HEU and LEU cores, respectively.

The radial power distributions demonstrate the difference between the HEU and LEU cores. As is shown in Table 3.9, the maximum half- element power at SU increases from 427 kW to 449 kW when going from HEU to LEU fuel (0.33 MW x relative power in Figures 3.12 and 3.13) At EOC there is a decrease in the maximum half-element power. The location of the maximum power is also given in the table.

There are two plena in the NBSR dividing the coolant flow between the six innermost fuel elements and the other 24 fuel elements. As is shown in Table 3.10, there is an 8.4% increase in the power in the innermost six fuel elements (FEs) at SU when going from HEU to LEU fuel and at EOC there is an 11% increase, though the total power generated by the inner six FEs is smaller at EOC than at SU. This indicates that when converting from HEU to LEU fuel, there is a net power shift from the perimeter of the core towards the inner portion of the core.

At SU there is more power generated in the lower half of the core than there is in the upper half of the core. This is due to the shim arms suppressing the power in the upper half of the core at SU. Because there is more power generated in the lower half of the core than there is in the upper half of the core starting at SU, the burnup is initially reduced in the upper half of the core. By the time the shim arms are swung out of the core and the EOC is approached the power is shifted to the upper half of the core as is demonstrated in Table 3.11.

A model of the NBSR was developed where the fuel elements were divided into 2x2 cm (nominally) squares. The number of fissions, which is proportional to the local power density, was calculated for each square. Thermal-hydraulic analyses are to be performed using these three-dimensional power distributions to ensure the reactor can be safely operated with the LEU fuel at all points in the fuel cycle.

Table 3.9 Highest Half-Element Power (kW)

	SU		EOC	
HEU	I2 Lower	427	H1 Upper	393
LEU	F3 Lower	449	H3 Upper	385

Table 3.10 Power (MW) Generated by the Inner Plenum FEs vs. the Outer Plenum FEs

	SU			EOC		
	HEU	LEU	Δ(%) HEU to LEU	HEU	LEU	Δ(%) HEU to LEU
Outer 24	16.00	15.64	-2.1%	16.18	15.76	-2.6%
Inner 6	4.00	4.34	8.4%	3.82	4.24	11.1%

Table 3.11 Power (MW) Generated in the Upper Half vs. the Lower Half of the Core

	SU			EOC		
	HEU	LEU	Δ(%) HEU to LEU	HEU	LEU	Δ(%) HEU to LEU
Upper	8.4	8.5	0.9	10.6	10.6	-0.2
Lower	11.6	11.5	-0.6	9.4	9.4	0.2

3.9 Figure-of-Merit for the Neutron Beams

The main purpose of the NBSR is to provide neutron beams for scientific research. The impact of the conversion on neutron beam performance needs to be assessed. Four locations were selected in the existing cold neutron source (CNS) and one location in each of the beam tubes 1, 4, 7, and 9 were selected to calculate the neutron flux passing through the selected locations. The fluxes were calculated at those locations and values from the LEU fueled core were compared to the values for the HEU core. The values were averaged with the locations in the CNS given double weight. The comparison is then the percent difference between the results for the HEU and the results for the LEU fuel. It is referred to as the figure-of-merit, FOM. The FOM for the LEU fuel at SU is 92% and at EOC is 90%. Hence, the conversion to LEU represents approximately a 10% decline in neutron beam performance for experimenters.

3.10 Effect of Dropping the Coolant to the Dump Level

The NBSR has a pipe, referred to as the moderator dump, whose entrance is just above the fueled portion of the core. If an emergency situation requires it, the pipe can be used to drain the coolant to that dump level leaving the core with no upper reflector. The lack of an upper reflector should result in the reactor becoming subcritical. The NBSR model was modified so that the coolant above the core could be changed as is shown in Figure 3.16. In this figure the area above the fueled portion of the core is devoid of coolant. Calculations of the k_{eff} when the coolant is lowered to the dump level were performed for the case that the shim arms and regulating rod were fully withdrawn. These results are shown in Table 3.12 and demonstrate that the NBSR can be kept subcritical under all conditions if the coolant were to be lowered to the dump level.

Table 3.12 Value of k_{eff} when the Coolant Is Lowered to the Dump Level

	HEU	LEU
SU	0.98572 ± 0.00044	0.98491 ± 0.00029
EOC	0.91241 ± 0.00029	0.92150 ± 0.00028

3.11 Beam Tube Flooding

Beam tube flooding was hypothesized to occur if a D_2O cooled experiment in a beam tube were to leak, or a crack were to occur in a beam tube, a thimble, or the cold neutron source. Such an event would allow D_2O to enter areas that are normally filled with air or vacuum and introduce a positive reactivity. The three situations calculated for the SAR are reproduced in Table 3.13. As can be seen from the table, the reactivity added is less than the 0.5 %Δk/k used to analyze the maximum reactivity insertion accident in the SAR.

Table 3.13 Reactivity Insertion (%Δk/k) from Flooding the Beam Tubes

	SU		EOC	
	HEU	LEU	HEU	LEU
CNS Flooded	0.24%	0.15%	0.25%	0.15%
Average Radial Beam Tube	0.17%	0.17%	0.18%	0.17%
One Tangential Beam Tube	0.27%	0.26%	0.20%	0.26%

3.12 Light Water Ingress

The NBSR is a D_2O cooled and moderated system. The D_2O is 99.97% pure. Any light water contamination would have a negative effect on the operability of the NBSR which is shown in Figures 3.17 and 3.18.

3.13 Fuel Misloading Accident

The fuel misloading accident is analyzed assuming a fresh, unirradiated fuel element is inserted into an incorrect location. This might cause a power level in that fuel element that could be unacceptable in terms of thermal limits. In order to perform this analysis, one fuel element was placed in each position in the core and the fuel element that should have been placed in that location is placed in the A4 position (one of the four positions for fresh fuel element). The radial power distributions were calculated at SU,

the limiting condition. The half-element with the maximum relative power was determined and the location and relative power are given in Table 3.14. The first column is the location in which the fresh fuel element was placed, the second and fourth columns show the location which exhibited the highest relative power and the third and fifth columns show the relative power (unity represents 20 MW / 60 materials) in the location.

For the HEU fuel the highest power occurred when the fresh fuel element was placed in the F3 location and for the LEU fuel the highest power occurred in the H3 location. Figure 3.19 shows the radial power distribution for the fresh HEU fuel element placed in the F3 position and Figure 3.20 shows the radial power distribution for the fresh LEU fuel element placed in the H3 position. For those two situations, a full three-dimensional power distribution analysis was performed.

Table 3.14 Maximum Relative Power in the Lower Half of the FEs for a Misloaded FE at SU

	HEU		LEU	
	Max FE	Max PD	Max FE	Max PD
normal	F3	1.23	H3	1.35
Swap fresh FE with:				
F1	I2	1.29	F3	1.35
B3	B3	1.39	H3	1.36
C6	C6	1.34	H3	1.34
E2	E2	1.66	E2	1.54
E6	E6	1.56	E6	1.48
E4	E4	1.91	E4	1.81
D7	H3	1.27	H3	1.35
C2	C2	1.37	F3	1.35
B5	B5	1.43	B5	1.36
F7	F7	1.30	H3	1.32
C4	C4	1.68	C4	1.56
F3	F3	1.93	F3	1.83
F5	F5	1.87	F5	1.80
H1	I2	1.30	H3	1.35
L3	L3	1.38	F3	1.36
K6	K6	1.34	H3	1.35
I2	I2	1.66	I2	1.54
I6	I6	1.55	I6	1.48
I4	I4	1.89	I4	1.79
J7	H3	1.27	F3	1.34
K2	K2	1.39	H3	1.35
L5	L5	1.38	H3	1.35
H7	H7	1.33	F3	1.33
K4	K4	1.62	K4	1.53
H3	H3	1.92	H3	1.83
H5	H5	1.87	H5	1.80

	A	B	C	D	E	F	G	H	I	J	K	L	M
				COLD SOURCE									
1				30.2		33.2		34.8		32.3			
2			33.4		34.3		<>		34.5		34.2		
3		32.8		<>		33.4		33.5		<>		33.7	
4	32.6		31.4		32.4		<>		32.0		30.8		32.6
5		31.9		<>		28.2		27.8		<>		30.9	
6			31.3		30.3		<RR>		30.3		30.6		
7				31.1		29.5		29.2		31.1			

Figure 3.1 Grams of ^{235}U Burned per Fuel Element per cycle, for HEU Fuel.

	A	B	C	D	E	F	G	H	I	J	K	L	M
				COLD SOURCE									
1				27.5		30.2		31.9		30.7			
2			30.9		32.4		<>		33.3		31.1		
3		31.4		<>		33.8		33.6		<>		31.8	
4	30.7		30.6		32.5		<>		32.5		30.2		30.7
5		30.5		<>		29.4		29.1		<>		28.9	
6			29.5		30.0		<RR>		29.6		29.3		
7				29.9		28.3		28.2		30.1			

Figure 3.2 Grams of ^{235}U Burned per Fuel Element per cycle, for LEU Fuel.

	A	B	C	D	E	F	G	H	I	J	K	L	M
				COLD SOURCE									
1				2.7		3.1		2.9		1.6			
2			2.5		1.9		<>		1.2		3.1		
3		1.4		<>		-0.4		-0.1		<>		1.9	
4	1.9		0.8		-0.1		<>		-0.5		0.6		1.8
5		1.4		<>		-1.2		-1.4		<>		2.0	
6			1.8		0.4		<RR>		0.7		1.3		
7				1.2		1.1		0.9		1.0			

Figure 3.3 Difference in the ^{235}U Burn Between HEU and LEU Fuels.

	A	B	C	D	E	F	G	H	I	J	K	L	M
				COLD SOURCE									
1				0.04		0.11		0.12		0.05			
2			0.18		0.34		<>		0.34		0.18		
3		0.18		<>		0.50		0.49		<>		0.18	
4	0.05		0.40		0.52		<>		0.53		0.41		0.04
5		0.25		<>		0.59		0.60		<>		0.25	
6			0.26		0.43		<RR>		0.44		0.26		
7				0.11		0.31		0.32		0.11			

Figure 3.4. Contribution to the Power (%) from the Fissioning of ^{239}Pu in Each Fuel Element for HEU Fuel at EOC.

	A	B	C	D	E	F	G	H	I	J	K	L	M
				COLD SOURCE									
1				0.55		1.50		1.47		0.58			
2			2.28		4.36		<>		4.39		2.32		
3		2.37		<>		6.24		6.35		<>		2.44	
4	0.56		5.14		6.53		<>		6.54		5.16		0.59
5		3.16		<>		7.46		7.49		<>		3.17	
6			3.29		5.46		<RR>		5.52		3.31		
7				1.38		4.00		4.02		1.40			

Figure 3.5. Contribution to the Power (%) from the Fissioning of ^{239}Pu in Each Fuel Element for LEU Fuel at EOC.

	A	B	C	D	E	F	G	H	I	J	K	L	M
				COLD SOURCE									
1				0.00		0.01		0.01		0.00			
2			0.02		0.05		<>		0.05		0.02		
3		0.02		<>		0.11		0.11		<>		0.02	
4	0.00		0.07		0.12		<>		0.12		0.07		0.00
5		0.03		<>		0.16		0.16		<>		0.03	
6			0.03		0.08		<RR>		0.08		0.03		
7				0.01		0.04		0.04		0.01			

Figure 3.6 Contribution to the Power (%) from the Fissioning of the Other Actinides in Each Fuel Element for HEU Fuel at EOC.

	A	B	C	D	E	F	G	H	I	J	K	L	M
				COLD SOURCE									
1				0.00		0.02		0.02		0.00			
2			0.05		0.24		<>		0.25		0.05		
3		0.05		<>		0.62		0.64		<>		0.05	
4	0.00		0.37		0.68		<>		0.70		0.37		0.00
5		0.11		<>		0.97		0.96		<>		0.11	
6			0.12		0.42		<RR>		0.44		0.12		
7				0.01		0.20		0.20		0.02			

Figure 3.7. Contribution to the Power (%) from the Fissioning of the Other Actinides in Each fuel Element for LEU Fuel at EOC.

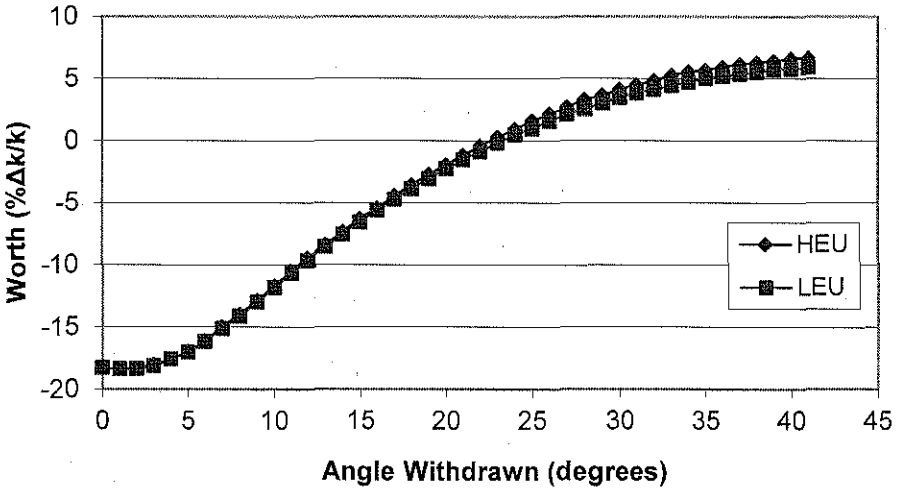

Figure 3.8 HEU and LEU Shim Arm Worth at SU

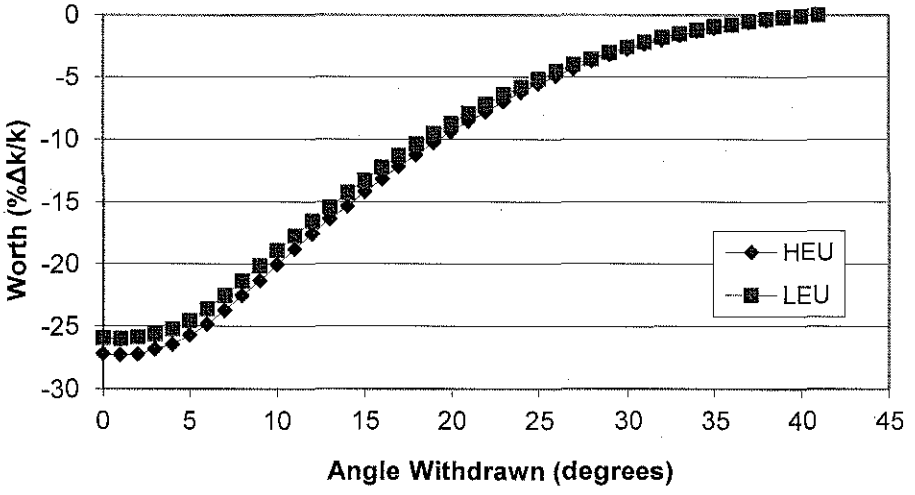

Figure 3.9 HEU and LEU Shim Arm Worth at EOC

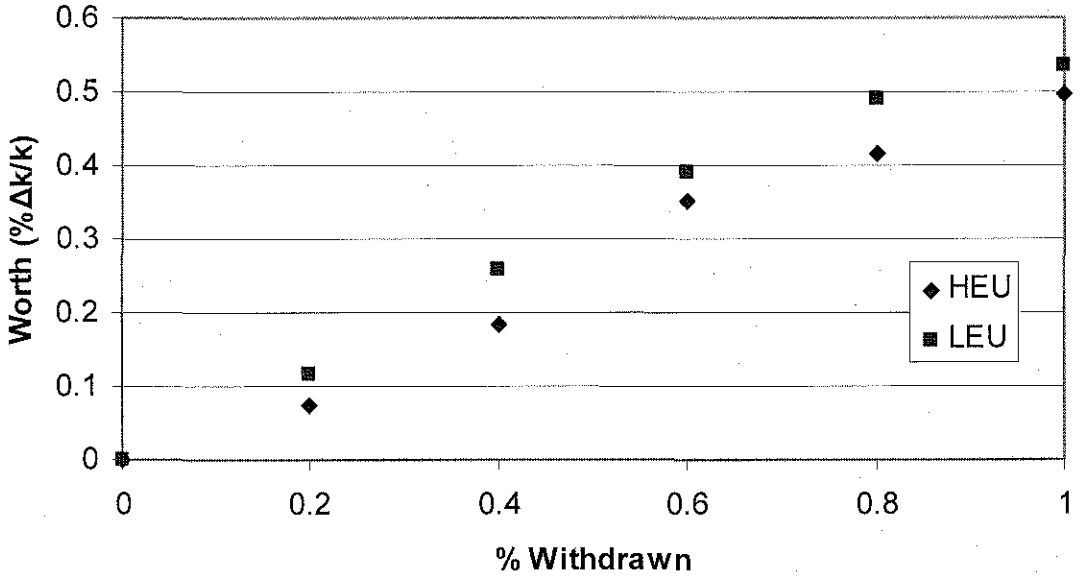

Figure 3.10 Regulating Rod Worth at SU for HEU and LEU Fuels

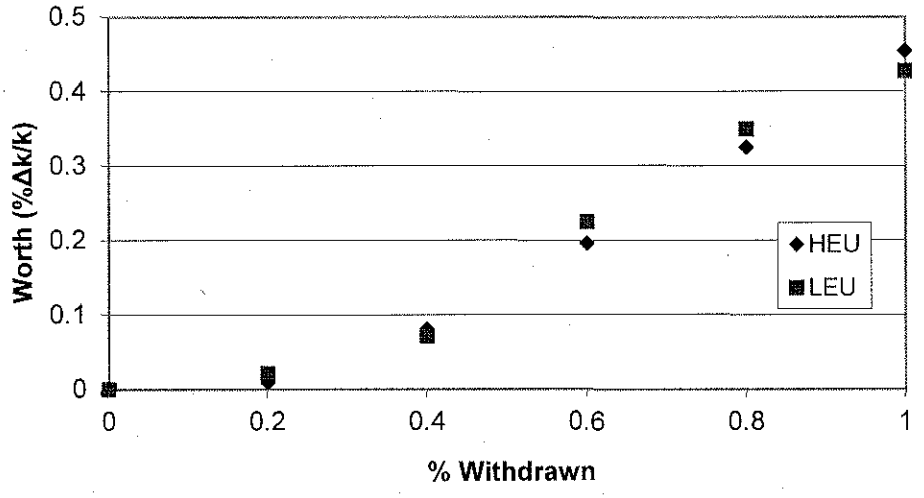

Figure 3.11 Regulating Rod Worth at EOC for HEU and LEU Fuels

Upper Core

	A	B	C	D	E	F	G	H	I	J	K	L	M
					COLD SOURCE								
1				0.98		1.05		1.11		0.99			
2			0.95		1.02		<>		0.95		0.82		
3		0.74		<>		0.91		0.90		<>		0.72	
4	0.64		0.71		0.82		<>		0.81		0.70		0.64
5		0.66		<>		0.74		0.74		<>		0.68	
6			0.72		0.80		<RR>		0.86		0.85		
7				0.91		0.91		0.92		0.97			

Lower core

	A	B	C	D	E	F	G	H	I	J	K	L	M
					COLD SOURCE								
1				1.07		1.17		1.23		1.14			
2			1.24		1.27		<>		1.28		1.26		
3		1.25		<>		1.27		1.27		<>		1.24	
4	1.24		1.19		1.22		<>		1.21		1.15		1.20
5		1.20		<>		1.05		1.04		<>		1.15	
6			1.12		1.09		<RR>		1.08		1.10		
7				1.04		0.99		0.99		1.03			

Figure 3.12 Radial Power Distribution for the Upper and Lower Halves of the HEU Core at SU.

Upper Core

	A	B	C	D	E	F	G	H	I	J	K	L	M
					COLD SOURCE								
1				0.90		1.01		1.05		0.93			
2			0.91		1.01		<>		0.94		0.78		
3		0.71		<>		0.97		0.96		<>		0.69	
4	0.61		0.73		0.89		<>		0.89		0.74		0.62
5		0.66		<>		0.84		0.85		<>		0.69	
6			0.72		0.84		<RR>		0.91		0.87		
7				0.89		0.91		0.94		0.96			

Lower core

	A	B	C	D	E	F	G	H	I	J	K	L	M
					COLD SOURCE								
1				0.98		1.09		1.15		1.05			
2			1.18		1.25		<>		1.27		1.19		
3		1.20		<>		1.35		1.34		<>		1.19	
4	1.15		1.21		1.30		<>		1.30		1.18		1.13
5		1.16		<>		1.17		1.16		<>		1.12	
6			1.10		1.13		<RR>		1.12		1.10		
7				1.00		1.01		1.00		1.01			

Figure 3.13 Radial Power Distribution for the Upper and Lower Halves of the LEU Core at SU.

Upper Core

	A	B	C	D	E	F	G	H	I	J	K	L	M
						COLD SOURCE							
1				1.00		1.11		1.18		1.11			
2			1.08		1.11		<>		1.14		1.16		
3		1.09		<>		1.07		1.07		<>		1.16	
4	1.10		1.03		1.04		<>		1.04		1.03		1.11
5		1.08		<>		0.91		0.91		<>		1.03	
6			1.07		1.02		<RR>		1.01		1.02		
7				1.08		1.01		0.99		1.05			

Lower core

	A	B	C	D	E	F	G	H	I	J	K	L	M
						COLD SOURCE							
1				0.85		0.93		0.97		0.91			
2			0.99		0.98		<>		1.00		1.02		
3		1.02		<>		0.96		0.97		<>		1.03	
4	1.05		0.96		0.94		<>		0.92		0.93		1.02
5		1.01		<>		0.82		0.81		<>		0.96	
6			0.94		0.90		<RR>		0.88		0.92		
7				0.90		0.87		0.85		0.89			

Figure 3.14 Radial Power Distribution for the Upper and Lower Halves of the HEU Core at EOC.

Upper Core

	A	B	C	D	E	F	G	H	I	J	K	L	M
						COLD SOURCE							
1				0.93		1.04		1.09		1.02			
2			1.04		1.11		<>		1.13		1.09		
3		1.04		<>		1.15		1.15		<>		1.10	
4	1.02		1.06		1.14		<>		1.14		1.05		1.03
5		1.05		<>		1.05		1.04		<>		1.01	
6			1.05		1.06		<RR>		1.05		1.01		
7				1.03		1.02		1.01		1.01			

Lower core

	A	B	C	D	E	F	G	H	I	J	K	L	M
						COLD SOURCE							
1				0.78		0.86		0.91		0.84			
2			0.94		0.98		<>		1.00		0.97		
3		0.98		<>		1.04		1.04		<>		0.98	
4	0.97		0.98		1.03		<>		1.02		0.96		0.95
5		0.98		<>		0.96		0.95		<>		0.94	
6			0.94		0.96		<RR>		0.94		0.91		
7				0.87		0.87		0.86		0.85			

Figure 3.15 Radial Power Distribution for the Upper and Lower Halves of the LEU Core at EOC.

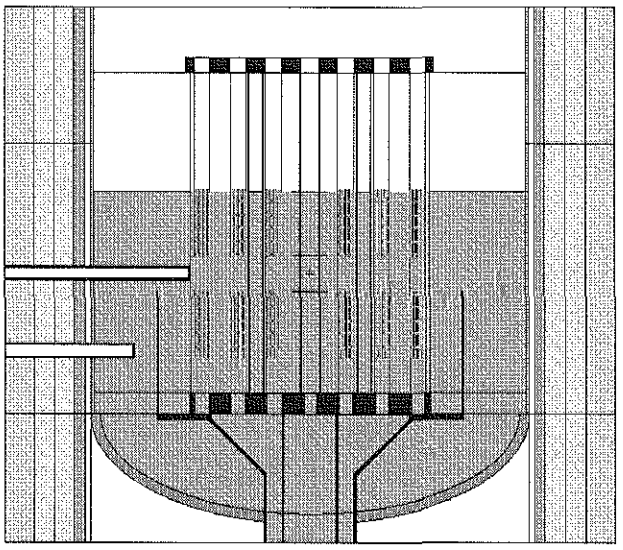

Figure 3.16 Vertical Section of the NBSR with the Coolant Dropped to the Dump Level.

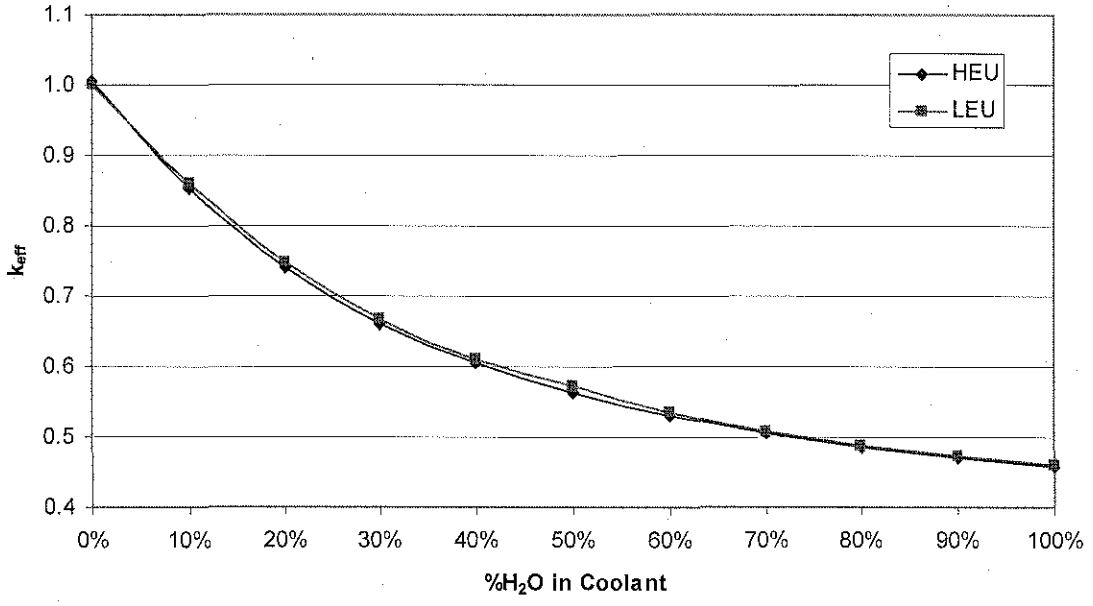

Figure 3.17 Effect of Light Water Ingress on the Value of k_{eff} at SU.

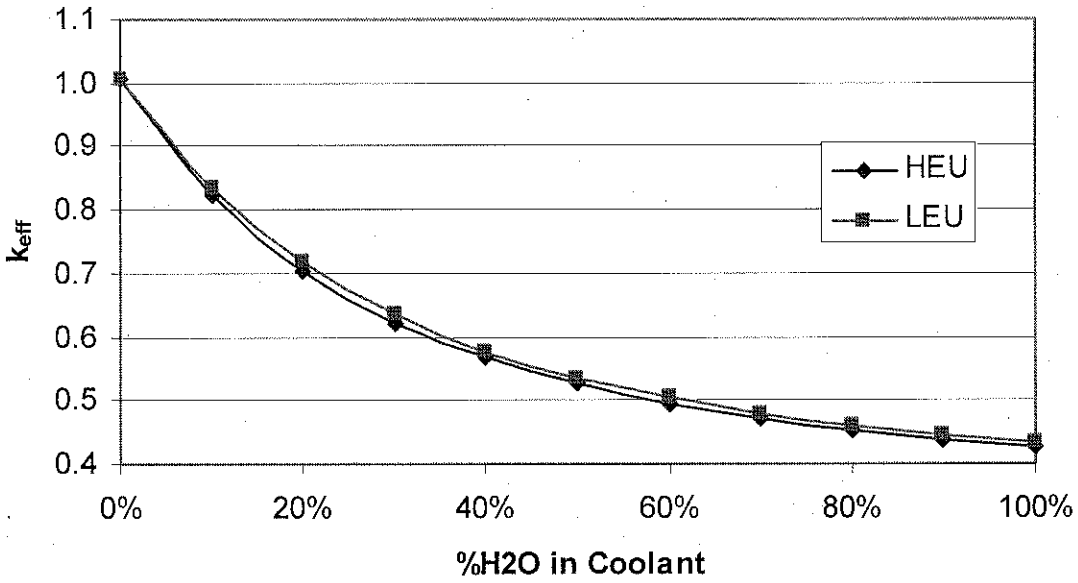

Figure 3.18 Effect of Light Water Ingress on the Value of k_{eff} at EOC.

Upper Core

	A	B	C	D	E	F	G	H	I	J	K	L	M
					COLD SOURCE								
1				0.63		1.04		1.11		0.98			
2			0.94		1.01		<>		0.94		0.80		
3		0.74		<>		1.38		0.91		<>		0.70	
4	0.64		0.72		0.83		<>		0.83		0.71		0.63
5		0.65		<>		0.74		0.74		<>		0.68	
6			0.71		0.79		<RR>		0.86		0.84		
7				0.88		0.88		0.88		0.94			

Lower core

	A	B	C	D	E	F	G	H	I	J	K	L	M
					COLD SOURCE								
1				0.70		1.16		1.22		1.12			
2			1.22		1.28		<>		1.29		1.23		
3		1.24		<>		1.93		1.30		<>		1.22	
4	1.25		1.22		1.24		<>		1.21		1.15		1.17
5		1.18		<>		1.06		1.04		<>		1.13	
6			1.09		1.07		<RR>		1.06		1.08		
7				1.02		0.97		0.97		1.02			

Figure 3.19 Radial Power Distribution When the Fresh HEU Fuel Element is Placed in the F3 Position.

Upper Core

	A	B	C	D	E	F	G	H	I	J	K	L	M
					COLD SOURCE								
1				0.90		0.99		1.02		0.66			
2			0.92		1.01		<>		0.93		0.76		
3		0.72		<>		0.98		1.30		<>		0.68	
4	0.60		0.73		0.91		<>		0.90		0.73		0.60
5		0.65		<>		0.85		0.85		<>		0.68	
6			0.71		0.82		<RR>		0.89		0.85		
7				0.87		0.91		0.92		0.93			

Lower core

	A	B	C	D	E	F	G	H	I	J	K	L	M
					COLD SOURCE								
1				0.98		1.08		1.14		0.76			
2			1.17		1.27		<>		1.27		1.17		
3		1.18		<>		1.37		1.83		<>		1.17	
4	1.14		1.20		1.32		<>		1.34		1.18		1.13
5		1.15		<>		1.18		1.18		<>		1.13	
6			1.08		1.12		<RR>		1.13		1.09		
7				1.00		0.99		1.00		0.99			

Figure 3.20 Radial Power Distribution When the Fresh LEU Fuel Element is Placed in the H3 Position.

4. CONCLUSIONS

The MCNPX computer code with the BURN option was used to calculate the fuel composition for the NBSR when fueled with either HEU or LEU fuel. Neutronic parameters were then calculated for both of these equilibrium cores at different times during a fuel cycle. The results showed differences between the HEU and LEU cores that would not lead to any significant changes in the safety analysis for the converted core and were reasonable except for the change in neutrons that are to be provided to experimentalists. Indeed, calculations of the figure-of-merit for providing neutrons shows a decrease in performance of approximately 10% throughout the cycle.

The calculated delayed neutron fraction decreased slightly in going from HEU to LEU and this is consistent with the additional amount of fissions from ^{239}Pu that take place in the LEU core. Neutron lifetime calculations showed some anomalies but are consistent with the large uncertainty associated with the calculation. Reactivity coefficients for moderator temperature and void changes did not change significantly nor did the reactivity effect of dropping the coolant to the dump level, beam tube flooding or light water ingress. Total shim arm worth was not significantly changed and since both types of cores would have to have similar excess reactivity to run the same fuel cycle length, both cores showed similar shutdown margin (calculated with each of the four shim arms assumed out of the core).

Power distributions were also calculated through a fuel cycle. A comparison of the power in half-element sections of fuel elements showed significant differences in that the HEU core had its highest fuel element powers at the core periphery whereas the LEU core has the power peaking in the center. This is detrimental to providing neutrons to experimentalists through the various beam tubes. There was also an increase in the maximum half-element power in the LEU core at startup relative to that for the HEU core. The effect on the thermal-hydraulics has been checked in preliminary calculations that are still ongoing and has been found to be not limiting. The effect on power of a misloaded fuel element has been calculated to be greater in the LEU core and again, thermal-hydraulic analyses in the future will determine to what extent margin to thermal-hydraulic limits may have been reduced.

5. REFERENCES

1. A.L. Hanson and D.J. Diamond, "Calculation of Design Parameters for the HEU-to-LEU Conversion of the NBSR", Technical Report to the National Nuclear Security Administration and the National Institute of Standards and Technology, October 29, 2010.

2. NBSR14, "Safety Analysis Report", NISTIR 7102, NIST Center for Neutron Research, April 2004.

3. A.L. Hanson and D.J. Diamond, "Determination of Inventories and Power Distributions for the NBSR", Presented at the TRTR/IGORR Joint Meeting, Gaithersburg, MD, September 12-16, 2005.

4. D.I. Poston and H.R. Trellue, MONTEBURNS, Version 2.0, Los Alamos National Laboratory, updated Dec. 2, 2002.

5. "MCNP – A General Monte Carlo N-Particle Transport Code, Version 5", LA-UR-03-1987, Los Alamos National Laboratory, April 24, 2003.

6. S. Ludwig, "Revision to ORIGEN2 – Version 2.2," Oak Ridge National Laboratory, May 23, 2002.

7. D.B. Pelowitz, Ed., MCNPX User's Manual version 2.6.0, LANL report, LA-CP-07-1473, April, 2008.

8. W.B Wilson, T.R. England, M. Herman, R.E. MacFarland, and D.W. Muir, "Cinder'90 Code for Transmutation Calculations", LANL Report, LA-UR-97-2655, 1997.

9 A.L. Hanson and D.J. Diamond, "Calculation of Inventories, Power Distributions and Neutronic Parameters for the NBSR Using MCNPX," Presented at the TRTR/IGORR Joint Meeting, Knoxville, TN, September 19-23, 2010.

10 J. Bess, "September 2011 Status Update for the NRAD Reactor Benchmark Models," Presented at the TRTR Meeting, Idaho Falls, ID, September 13-15, 2011.

11 J. Stevens "GTRI Convert USHPRR Program, Reactor Conversion" Presented at the Reduced Enrichment Program for U.S. High Performance Reactors Meeting, July 27, 2011.

12 A.L. Hanson, H. Ludewig, and D.J. Diamond, "Calculation of the Prompt Neutron Lifetime in the NBSR", *Nuclear Science and Engineering, 153,* 2006.

13. B.C. Kiedrowski, T.E. Booth, F.B. Brown, J.A. Favorite, R.A. Forster, R.L. Martz, "MCNP5-1.6 Feature Enhancements and Manual Clarifications," LA-UR-10-06217.

14. J. Wang, and W.D. Reece, "Comparison of Different Numerical Methods Used in Delayed Neutron Decay Parameters Estimation," *Nuclear Science and Engineering, 167,* 2011.